Journal of Oral Health and Biosciences 34(2):34 ~ 39, 2022

Original Article

Volume Magnetic Susceptibility Estimation of α- and β-Phases in Titanium Alloys for Biomedical Applications

Muneyuki YOSHIMURA[1)], Emi UYAMA[2)], Kazumitsu SEKINE[2)], Shinya HORIUCHI[1)], Eiji TANAKA[1)], Kenichi HAMADA[2)]

Keywords: Volume magnetic susceptibility, Phase constitution, Heat treatment, Ti-6Al-4V alloy, Ti-Mo alloy

Abstract: Metallic medical devices in the human body cause serious artifacts in magnetic resonance imaging owing to the volume magnetic susceptibility (χ_v) mismatch between the device and tissue around the device. To reduce artifacts, medical devices produced from alloys with χ_v values of approximately -9×10^{-6} are required. Controlling the phase constitution is a basic technique used to control the χ_v value of an alloy, and the χ_v value of each phase is a fundamental property. In this study, an α+β-type Ti alloy and two β-type Ti alloys were investigated. The estimated χ_v values of the α-phase of the alloys were similar to or smaller than that of pure Ti. In contrast, the estimated χ_v values of the β-phase of the alloys were larger than that of pure Ti. Since the χ_v value of pure Ti is much larger than -9×10^{-6}, the χ_v values of the β-phases suggested that increasing the volume fraction of the β-phase was not appropriate for producing a Ti alloy with a lower χ_v value.

1. Introduction

Over the past few decades, magnetic resonance imaging (MRI) has been developed and improved. Currently, it is indispensable for minimally invasive diagnostic examination of the internal body. One of the major disadvantages of MRI compared to other imaging techniques is the imaging artifacts caused by the magnetization of metallic medical devices in a body[1)]. A volume magnetic susceptibility (χ_v) mismatch between the device and tissue surrounding the device causes a metal artifact in MR images. Since the χ_v value of human tissue is reported to be approximately -9×10^{-6}, metal materials for MRI-compatible devices must have χ_v values close to -9×10^{-6}. The metal element with a χ_v value closest to -9×10^{-6} is Cu (-9.63×10^{-6}) and the second closest is Ge (-7.1×10^{-6}), which is inappropriate for biomedical applications owing to its low corrosion resistance. In contrast, metal elements with a high corrosion resistance and excellent biocompatibility exhibit χ_v values much different from -9×10^{-6}, such as Ti (182×10^{-6}), Zr (100×10^{-6}), Nb (237×10^{-6}), and Ta (178×10^{-6}). The χ_v value of Au (-34×10^{-6}) is closer to the ideal χ_v value and exhibits a high corrosion resistance. However, its poor mechanical properties restrict its application. Therefore, new alloys with MRI compatibility must be developed to replace pure metal materials. We previously developed Au-based alloys with negative χ_v values very close to -9×10^{-6}, which is the ideal value[2, 3)]. Since their mechanical properties were improved, these alloys are considered as potential candidates for future biomedical

[1)] Department of Orthodontics and Dentofacial Orthopedics, Tokushima University Graduate School of Biomedical Sciences
[2)] Department of Biomaterials and Bioengineering, Tokushima University Graduate School of Biomedical Sciences

Table 1 Composition of Ti alloys

Material	Size, inch	Type	Composition, mass%	Manufacturer
TiMO	0.016 × 0.022	β	Ti-11Mo-6Zr-4Sn	Dentsply Sirona, USA
TiNB	0.016 × 0.022	β	Ti-36Nb-2Ta-3Zr-0.3O (typical)	JM ORTHO, JAPAN
64Ti	0.016 × 0.022	α+β	Ti-6.8Al-4.2V	TP Orthodontics, USA

applications. However, their poor mechanical properties, material cost, and high density restrict their applications. In contrast, recently developed Nb- and Zr-based alloys exhibit relatively low material costs and densities, as well as excellent mechanical properties[4-18]. However, they exhibited positive χ_v values that were not sufficiently close to -9×10^{-6}. These results promote the development of other MRI-compatible alloys that are more suitable for various biomedical applications.

To design an alloy and control its properties, optimization of the alloy composition, phase constitution, and plastic working are required. The effects of these three factors on the χ_v value of Au- and Zr-based alloys have been investigated in the aforementioned studies[2, 8, 19]. However, the effects of alloy composition and plastic working on the χ_v values were complicated: the correlations between the χ_v values and composition or reduction in area were not necessarily linear. In contrast, we found a linear effect of phase constitution on the χ_v values[3]. Therefore, the χ_v values of the phases in an alloy are the basic data used for obtaining the desired χ_v value of the alloy. Nonetheless, the χ_v values of phases consisting of many types of alloys have not been evaluated and reported. Researchers have examined the effect of phase constitution change in Zr-Mo alloys on their χ_v values[14]. However, the χ_v values of the phases were not quantitatively or individually evaluated. Moreover, although Ti alloys are the most widely used alloys for clinical applications, to the best of our knowledge, no quantitative or individual evaluation of the χ_v value of phases consisting of Ti alloys has been carried out.

In this study, the χ_v value and phase constitution of an α+β-type Ti alloy and two β-type Ti alloys were investigated. The phase constitutions of the alloys were changed through heat treatment (HT), and the volume fraction of the β-phase (V_β) was analyzed. The χ_v value of each phase was calculated using a linear regression of the correlation between χ_v and V_β.

2. Materials and Methods

2.1. Specimen preparation

The alloys investigated are α+β-type Ti-6Al-4V alloy (64Ti), β-type Ti-Mo alloy (TiMO), and β-type Ti-Nb alloy (TiNB). They were supplied as commercial orthodontic straight wires with rectangular cross-sections of the same size. The details are summarized in Table 1. Note that the wires used in this study were adopted not as wires for specific applications but as alloy samples for various types applications. To change the phase constitutions, several HTs were performed at different temperatures: 800 ℃ for annealing of all alloys; 800 and 550 ℃ for solution treatment and TiMO aging; 800 ℃ for TiNB aging; and 1100, 1050, and 550 ℃ for 64Ti aging. All HTs were performed in a quartz tube under vacuum (under ≈1×10^{-3} Pa), and the specimen was quenched by immersing the tube in water.

2.2. Vickers hardness

To remove potential plastic deformation during wire processing before evaluation, all specimens were fully annealed until the Vickers hardness (Hv) reduction was saturated with increasing annealing time. The Hv evaluation was performed with a load of 100 g for 30 s. The Hv was measured nine times for each specimen, and the mean value was calculated from the middle seven data points.

2.3. Magnetic susceptibility

The χ_v values were measured using a magnetic susceptibility balance (MSB-AUTO, Sherwood Scientific Ltd., UK) at room temperature (RT). Herein, 40-60 pieces of each specimen (less than 8 mm long) were placed in the specimen holder (3.24 mm inner diameter) with the longitudinal direction vertical to the magnetic field. χ_v was measured 30 times for each specimen, and the mean value and standard deviation (SD) were calculated for each specimen.

2.4. Phase constitution

The phase constitution was analyzed using X-ray diffractometry (XRD) with a Cu Kα source at 30 kV and 15 mA. Herein, 8-10 wires with lengths of 5-10 mm were embedded in an acrylic resin, and the cross section was polished with waterproof SiC paper (up to P4000) and a 1 nm diamond suspension. The XRD profile was analyzed using Fityk software (Fityk. ver. 1.3.1, (fityk.nieto.pl/)).

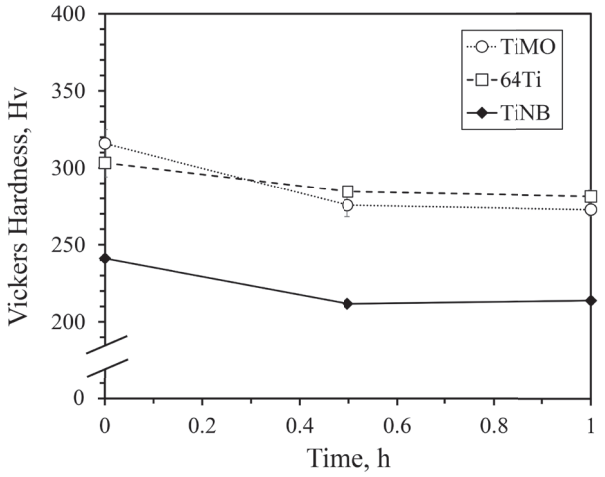

Fig. 1 Vickers hardness of TiMO, TiNB, and 64Ti annealed at 800 ℃

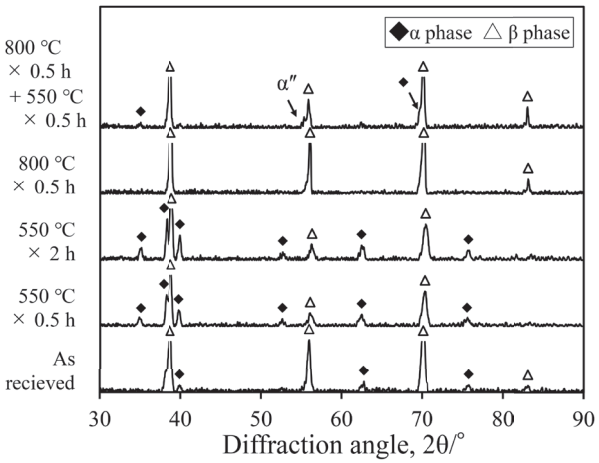

Fig. 2 XRD profiles of TiMO

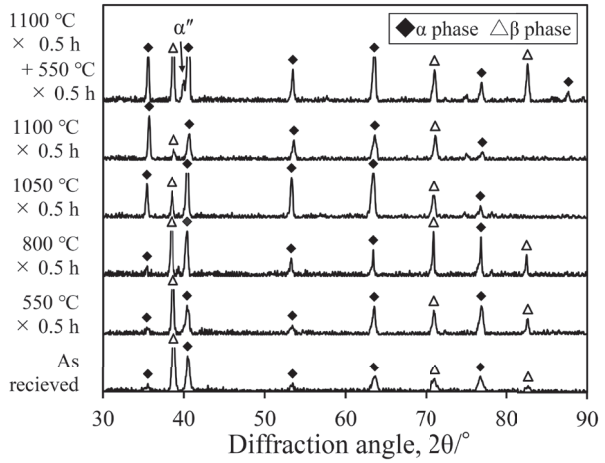

Fig. 3 XRD profiles of 64Ti

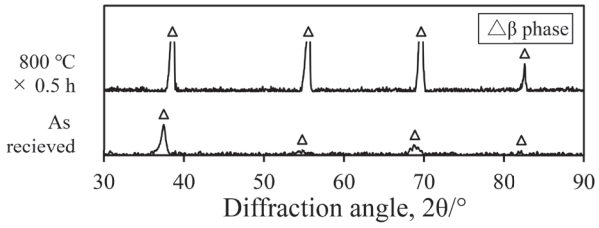

Fig. 4 XRD profiles of TiNB

3. Results

3.1. Vickers hardness

Fig. 1 shows the Hv values of the specimens. The Hv values of TiMO, TiNB, and 64Ti specimens before annealing were 315.9 (SD = 9.0), 303.3 (SD = 9.2), and 241.1 (SD = 2.0), respectively, whereas those after annealing at 800 ℃ for 0.5 h were 275.6 (SD = 7.4), 211.7 (SD = 7.0), and 284.5 (SD = 3.5), respectively. Since the Hv values after 1 h annealing did not change from those obtained after 0.5 h, a temperature of 800 ℃ and duration of 0.5 h were sufficient for full annealing.

3.2. Phase constitution

Fig. 2 shows the XRD profile of TiMO. Peaks corresponding to the β-phase (body-centered-cubic structure) and slight peaks corresponding to the α-phase (hexagonal structure) were observed in the as-received material. The peak intensity of the α-phase increased with HT time at 550 ℃. The slight peaks of the α-phase disappeared after annealing at 800 ℃ for 0.5 h, and they were observed again after subsequent aging at 500 ℃ for 0.5 h. In addition, the peak of the α”-phase (orthorhombic structure) was observed. Fig. 3 shows the XRD profile of 64Ti. Peaks corresponding to both the α- and β-phases were observed in all specimens before and after HTs. The slight peak of the α”-phase was observed only after HT at 1100 ℃ for 0.5 h followed by HT at 550 ℃ for 0.5 h. Fig. 4 shows the XRD profile of TiNB. Only the peaks of the β-phase were observed before and after HT; thus, TiNB did not show phase constitution changes. In this study, the ratios of the total β-phase peak area to the total peak area were calculated and are summarized as V_β in Table 2.

3.3. Magnetic susceptibility

The χ_v values of TiMO, TiNB, and 64Ti after annealing at 800 ℃ for 0.5 h were 261×10^{-6}, 279×10^{-6}, and 216×10^{-6},

Table 2 Volume fraction of β-phase of TiMO and 64Ti before and after HT

a) TiMO

Heat treatment	Volume fraction of β phase, %
as received	88.1
550 ℃ × 0.5 h	58.0
550 ℃ × 2 h	58.5
800 ℃ × 0.5 h	100.0
800℃ × 0.5 h + 550 ℃ × 0.5 h	63.3

b) 64Ti

Heat treatment	Volume fraction of β phase, %
as received	38.4
550 ℃ × 0.5 h	51.2
800 ℃ × 0.5 h	33.3
1050 ℃ × 0.5 h	8.2
1100 ℃ × 0.5 h	5.6
1100 ℃ × 0.5 h + 550 ℃ × 0.5 h	25.2

respectively. These values were higher than that of pure Ti. The χ_v values of each specimen after annealing at 800 ℃ for 0.5 h hardly changed compared to those before annealing. After aging at 550 ℃, the χ_v values of TiMO decreased to 212×10^{-6} (0.5 h) and 187×10^{-6} (2 h) with increasing aging time. In addition, after annealing at 800 ℃ for 0.5 h followed by aging at 550 ℃ for 0.5 h, the χ_v value was 220×10^{-6}. The χ_v values of 64Ti after annealing at 1050 and 1100 ℃ for 0.5 h were 193×10^{-6} and 185×10^{-6}, respectively, and that after aging at 550 ℃ for 0.5 h was 196×10^{-6}. After annealing at 1100 ℃ for 0.5 h followed by aging at 550 ℃ for 0.5 h, the χ_v value of 64Ti was 181×10^{-6}, which is close to that of pure Ti.

4. Discussion

4.1. Phase constitution of specimens

Although TiMO was supplied as a β-type alloy, the as-received alloy contained the β-phase mainly but also the α-phase slightly, *i.e.*, TiMO was the near β-type alloy. Since the α-phase could be eliminated after a short HT at 800 ℃, TiMO was designed to contain both the β- and α-phases to control its mechanical properties. The most important advantage of β-type alloys for biomedical applications is their low elastic modulus; however, β-type alloys generally exhibit lower strengths than α+β-type alloys. Therefore, the volume fraction of the α-phase is one of the key factors for optimizing the balance between strength and elastic modulus. In contrast, it was difficult to change the phase constitution of the TiNB alloy in this study. A previous study of Ti-Nb-Ta-Zr alloys showed that the α-phase precipitation with aging was dependent not only on the HT temperature but also on the oxygen content[20]. These data suggest that the HT temperature for TiNB was considerably high for aging, and a lower temperature (*e.g.*, lower than 500 ℃) and longer aging time were appropriate.

4.2. Effects of annealing on specimen properties

Annealing at 500 ℃ slightly reduced the Hv value of each specimen; that is, the work-hardening rate of each specimen was limited. Although the correlation between the work-hardening rate and plastic strain is not linear, the residual strain in each specimen was potentially small, which led to a lower effect of annealing on the χ_v values of each specimen. In addition, the plastic deformation of the specimen induced an anisotropy of χ_v. The wire specimen, which was used as-received, should possess anisotropy owing to the wire drawing in the process. However, owing to the small diameter of the wires, the anisotropy of χ_v could not be evaluated, but isotropic χ_v values were evaluated after full annealing.

4.3. V_β calculated from XRD profile

The volume fraction of each phase does not affect the intensity of the peaks but does affect the total peak area. Since the orientation of a crystal grain affects the intensity of a peak, a random orientation of grains is required for precise evaluation. The grains in the wire after wire drawing usually have an anisotropy of orientation parallel and vertical to the longitudinal direction of the wire. However, after full annealing, anisotropy is minimized, and the accuracy of the volume fraction evaluation should be improved.

In the evaluation of the β-phase volume fraction, the peak

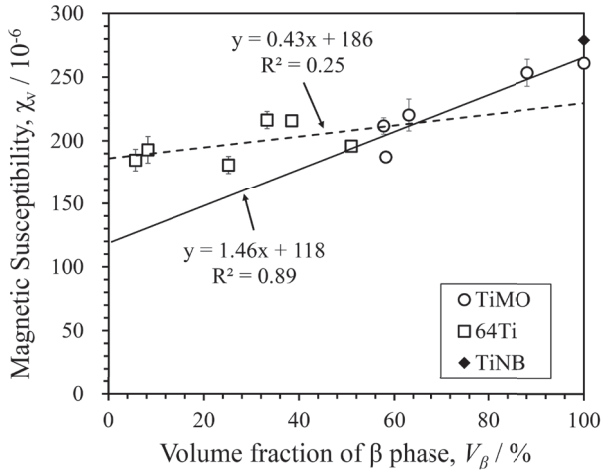

Fig. 5 Correlation between volume fraction of β-phase and volume magnetic susceptibility

signifying the α"-phase was ignored because the area was much smaller than those of the other peaks. In the case of ferromagnetic materials or phases, the χ_v value indicates an extreme increase with the detection of their small peak. However, the χ_v values of the specimens containing the α"-phase did not increase extraordinarily. Thus, the area of the α"-phase peak was negligible.

4.4. Correlation between V_β and χ_v values

Fig. 5 shows the correlation between the V_β and χ_v values. A linear regression of the data for TiMO and 64Ti indicated a positive dependence of the χ_v value on V_β. The χ_v value of the β-phase of the alloy was larger than that of the α-phase. Since pure Ti exhibits the α-phase at RT, the χ_v value of Ti (182×10^{-6}) is a reference for α-type Ti alloys and α-phases in Ti alloys. The estimated χ_v value of the α-phase of 64Ti was similar to this value. The χ_v value of the Ti-6Al-4V alloy reported previously was 190×10^{-6}, which is smaller than that of the as-received 64Ti[21]. The results obtained for 64Ti suggested that the V_β value of as-received 64Ti was larger than that reported previously. The χ_v value of the α-phase of TiMO was estimated to be smaller than those of pure Ti and 64Ti. One of the main reasons for this is the difference in the alloy compositions. However, because the content of an element in the alloy does not necessarily affect the χ_v value linearly, a quantitative analysis of the effect of the content on the χ_v value is difficult.

The χ_v value of the estimated β-phase of TiMO was similar to that of TiNB, and that of 64Ti was smaller than those of the other two alloys. However, each χ_v value of the β-phase was larger than that of pure Ti, that is, increasing the volume fraction of the β-phase was not appropriate for producing a Ti alloy with a χ_v value lower than that of pure Ti. In contrast, pure Zr, with the same α-phase (hexagonal structure) as Ti at RT, shows a larger χ_v value than that of the β-type Zr-15Mo alloy[14]. These inconsistent results suggest that the χ_v value of the β-phase of a Ti alloy is not necessarily larger than that of the α-phase; thus, the estimation of the χ_v value of both the α- and β-phases is required for other Ti alloys.

4.5. Future Work

Several other β-type Ti alloys and α+β-type Ti alloys for medical applications are listed in the ASTM Standards (ASTM International) or ISO Standard (International Organization for Standardization) as β-type Ti alloys, *i.e.*, Ti-13Nb-13Zr (ASTM F1713), Ti-12Mo-6Zr-2Fe (ASTM F1813), Ti-15Mo (ASTM F2066), and Ti-15Mo-5Zr-3Al (ISO 5832-14), and as an α+β type Ti alloy, namely Ti-6Al-7Nb (ASTM F1298/ ISO 5832-11). The estimation of χ_v values for both the α- and β-phases in these alloys will clarify not only the effect of the phase on the values but also the effect of the composition on these values. These data will contribute to the design of new β-type Ti alloys and α+β-type Ti alloys with χ_v values lower than that of pure Ti.

5. Conclusion

The χ_v values of an α+β-type Ti alloy and two β-type Ti alloys were investigated. The phase constitutions were changed through HT, and the χ_v values of the α- and β-phases were estimated individually. The χ_v values of the α-phase were similar to or smaller than those of pure Ti. In contrast, the χ_v values of the β-phase of the alloys were larger than those of pure Ti or α-type Ti alloys of the same composition. In conclusion, although the number of alloy types is limited, it is potentially difficult to produce a new β-type Ti alloy with χ_v value lower than that of pure Ti or α-type Ti alloy of the same composition.

Declaration of Competing Interest

The authors declare that they have no known competing financial interests or personal relationships that could have influenced the work reported in this study.

Acknowledgements

This study was partially supported by JSPS KAKENHI Grant Number 17H06904.

References

1） Schenck JF: The role of magnetic susceptibility in magnetic resonance imaging: MRI magnetic compatibility of the first and second kinds. Med Phys 23, 815-850 (1996)

2）Uyama E, Inui S, Hamada K, Honda E and Asaoka K: Magnetic susceptibility and hardness of Au-xPt-yNb alloys for biomedical applications. Acta Biomater 9, 8449-8453 (2013)
3）Inui S, Uyama E and Hamada K: Volume magnetic susceptibility design and hardness of Au-Ta alloys and Au-Nb alloys for MRI-compatible biomedical applications. Biomed Phys Eng Express 3, 015025 (2017)
4）O'Brien BJ, Stinson JS, Boismier DA and Carroll WM: Characterization of an NbTaWZr alloy designed for magnetic resonance angiography compatible stents. Biomaterials 29, 4540-4545 (2008)
5）O'Brien B, Stinson J and Carroll W: Development of a new niobium-based alloy for vascular stent applications. J Mech Behav Biomed Mater 1, 303-312 (2008)
6）Li HZ and Xu J: MRI compatible Nb-Ta-Zr alloys used for vascular stents: Optimization for mechanical properties. J Mech Behav Biomed Mater 32, 166-176 (2014)
7）Li XM, Li HZ, Wang SP, Huang HM, Huang HH, Ai HJ and Xu J: MRI-compatible Nb-60Ta-2Zr alloy used for vascular stents: Haemocompatibility and its correlation with protein adsorption. Mater Sci Eng C 42, 385-395 (2014)
8）Li HZ, Zhao X and Xu J: MRI-compatible Nb-60Ta-2Zr alloy for vascular stents: Electrochemical corrosion behavior in simulated plasma solution. Mater Sci Eng C 56, 205-214 (2015)
9）Kajima Y, Doi H, Takaichi A, Hanawa T and Wakabayashi N: Surface characteristics and castability of Zr-14Nb alloy dental castings. Dent Mater J 33, 631-637 (2014)
10）Kondo R, Nomura N, Suyalatu, Tsutsumi Y, Doi H and Hanawa T: Microstructure and mechanical properties of as-cast Zr-Nb alloys. Acta Biomater 7, 4278-4284 (2011)
11）Kondo R, Shimizu R, Nomura N, Doi H, Tsutsumi Y, Mitsuishi K, Shimojo M, Noda K and Hanawa T: Effect of cold rolling on the magnetic susceptibility of Zr-14Nb alloy. Acta Biomater 9, 5795-5801 (2013)
12）Nomura N, Tanaka Y, Suyalatu, Kondo R, Doi H, Tsutsumi Y and Hanawa T: Effects of Phase Constitution of Zr-Nb Alloys on Their Magnetic Susceptibilities. Mater Trans 50, 2466-2472 (2009)
13）Zhou F, Qiu K, Bian D, Zheng Y and Lin J: A Comparative in vitro Study on Biomedical Zr-2.5X (X= Nb, Sn) Alloys. J Mater Sci Technol 30, 299-306 (2014)
14）Suyalatu, Nomura N, Oya K, Tanaka Y, Kondo R, Doi H, Tsutsumi Y and Hanawa T: Microstructure and magnetic susceptibility of as-cast Zr-Mo alloys. Acta Biomater 6, 1033-1038 (2010)
15）Suyalatu, Kondo R, Tsutsumi Y, Doi H, Nomura N and Hanawa T: Effects of phase constitution on magnetic susceptibility and mechanical properties of Zr-rich Zr-Mo alloys. Acta Biomater 7, 4259-4266 (2011)
16）Zhou D-B, Wang S-P, Wang S-G, Ai H-J and Xu J: Bulk metallic glasses: MRI compatibility and its correlation with magnetic susceptibility. J Mater Sci Technol 32, 496-504 (2016)
17）Zhou DB, Wang SG, Wang SP, Ai HJ and Xu J: MRI compatibility of several early transition metal based alloys and its influencing factors. J Biomed Mater Res Part B Appl Biomater 106, 377-385 (2018)
18）Ashida M, Morita M, Tsutsumi Y, Nomura N, Chen P and Hanawa T: Effects of cold swaging on mechanical properties and magnetic susceptibility of the Zr-1Mo alloy. Metals 8, 454 (2018)
19）Johansson CH and Linde JO: Kristallstruktur, elektrischer Widerstand, Thermokräfte, Wärmeleitfähigkeit, magnetische Suszeptibilität, Härte und Vergütungserscheinungen des Systems Au Pt in Verbindung mit dem Zustandsdiagramm. Annalen der Physik 397, 762-792 (1930)
20）Nakai M, Niinomi M, Akahori T, Tsutsumi H and Ogawa M: Effect of oxygen content on microstructure and mechanical properties of biomedical Ti-29Nb-13Ta-4.6Zr alloy under solutionized and aged conditions. Mater Trans 50, 2716-2720 (2009)
21）Horton J and Parsell D: Biomedical potential of a zirconium-based bulk metallic glass. MRS Online Proceedings Library (OPL), 754 (2002)